Consequences of Broken Translational Symmetry in $FeSe_xTe_{1-x}$

L. Moreschini,[1,*] P.-H. Lin,[2,†] C.-H. Lin,[3,4] W. Ku,[3,4] D. Innocenti,[1,5] Y. J. Chang,[1,6,7] A. L. Walter,[1,6] K. S. Kim,[1] V. Brouet,[8] K.-W. Yeh,[9] M.-K. Wu,[10] E. Rotenberg,[1] A. Bostwick,[1] and M. Grioni[2]

[1]*Advanced Light Source (ALS), Lawrence Berkeley National Laboratory, Berkeley, California 94720, USA*
[2]*Ecole Polytechnique Fédérale de Lausanne (EPFL), Institute of Condensed Matter Physics, CH-1015 Lausanne, Switzerland*
[3]*Condensed Matter Physics and Materials Science Department, Brookhaven National Laboratory, Upton, New York 11973, USA*
[4]*Department of Physics and Astronomy, Stony Brook University, Stony Brook, New York 11794, USA*
[5]*CNR-SPIN and Dipartimento di Ingegneria Civile ed Ingegneria Informatica, University of Roma Tor Vergata, 00133 Rome, Italy*
[6]*Department of Physical Chemistry, Fritz-Haber-Institut der Max-Planck-Gesellschaft, Faradayweg 4-6, 14195 Berlin, Germany*
[7]*Department of Physics, University of Seoul, Seoul 130-743, Republic of Korea*
[8]*Laboratoire de Physique des Solides, Université Paris-Sud, UMR 8502, Bâtiment 510, 91405 Orsay, France*
[9]*Institute of Physics, Academia Sinica, 128 Section 2 Academia Road, Nankang, Taipei 11529, Taiwan*
[10]*Department of Physics, National Dong Hwa University, Hualien 97401, Taiwan*

(Received 23 October 2013; published 25 February 2014)

We investigate the consequences of broken translational symmetry in the superconductor $FeSe_xTe_{1-x}$ using angle-resolved photoemission spectroscopy. We find that the intensity does not follow the periodicity dictated by the crystal structure, owing to the form of the perturbing potential and the symmetries of the Fe d orbitals. Their interplay leads to substantial differences in the orbital character and spectral features observed at nominally equivalent locations in the reciprocal space. Such differences cannot be accounted for by the usual dipole matrix element effects and are due instead to the structure factor, which must be explicitly considered whenever more than one atom is present in the unit cell.

DOI: 10.1103/PhysRevLett.112.087602 PACS numbers: 79.60.-i, 71.90.+q, 74.25.Jb, 74.70.Ad

Quasiparticles (QPs), the elementary electronic excitations of a solid, are expected to reflect the periodicity of the underlying lattice. However, translational symmetry can be perturbed by disorder, or by a periodic structural distortion, or by the emergence of new order parameters, as in the case of magnetic, charge, or orbital order. The symmetry of the QP states is then modified, both in real space and in momentum space. The ideal tool to study how translational symmetry breaking affects the electrons in a crystal is angle-resolved photoemission spectroscopy (ARPES), which measures the momentum dependent one-particle spectral function $A(k, \omega)$, where k and ω are the QP momentum and energy.

Like all spectroscopies, ARPES measures excited final states. Nevertheless, in the absence of strong correlations, the photoemission intensity is usually interpreted as a picture of initial single-particle states. Such a conceptual shortcut is often useful, but is not always allowed. In particular, it can be misleading whenever multiple atoms in the unit cell lead to conflicting periodicities. For instance, if a given crystal structure is slightly modified by a perturbing potential, the initial states are forced to follow a new reduced Brillouin zone (BZ), whereas the ARPES intensity is hardly affected, and essentially follows the pristine periodicity [1]. Moreover, single-site orbitals are unfit to describe the electronic structure in a multisite unit cell [2]. As a result, not just an intensity modulation but clearly distinct spectral features may be observed in ARPES among the different BZs.

The superconducting iron pnictides and chalcogenides offer the possibility of investigating some of these unintuitive effects. All these materials contain square lattice planes of Fe ions. In the $FeSe_xTe_{1-x}$ alloy considered here, they are coordinated to Te(Se) ions located alternatively above and below the planes [Fig. 1(a)]. If the out-of-plane displacement of the Te(Se) ions were artificially reduced to zero, the tetragonal unit cell would contain one Fe atom (1-Fe), but the staggered chalcogen ions break this 1-Fe structural symmetry. Thus, the actual $(\sqrt{2} \times \sqrt{2})R45°$ unit cell contains 2 Fe atoms (2-Fe) and is rotated by 45° [Fig. 1(b)]. In the reciprocal space, the 2-Fe BZ is correspondingly smaller than the 1-Fe BZ, and also rotated by 45° [Fig. 1(c)]. This ambiguity in the definition of the unit cell has generated some confusion in the literature [3].

In this Letter, we show that an extended k-space survey reveals distinctive signatures of symmetry breaking in $FeSe_xTe_{1-x}$. Namely, we observe holelike Fermi surface (FS) sheets at the centers of all 2-Fe BZs, whose orbital character follows instead the 1-Fe periodicity, violating the symmetry of the reciprocal lattice. In particular, the characteristic hole pockets at Γ and M present opposite parity with respect to the plane containing the sample surface. This is a consequence of the peculiar form of the symmetry-breaking potential, which yields the same value for the nearest-neighbor hopping integrals for the two Fe sites, apart from a sign [5]. For the reliability of our conclusions, it is crucial to explore a sufficiently broad

 © 2014 American Physical Society

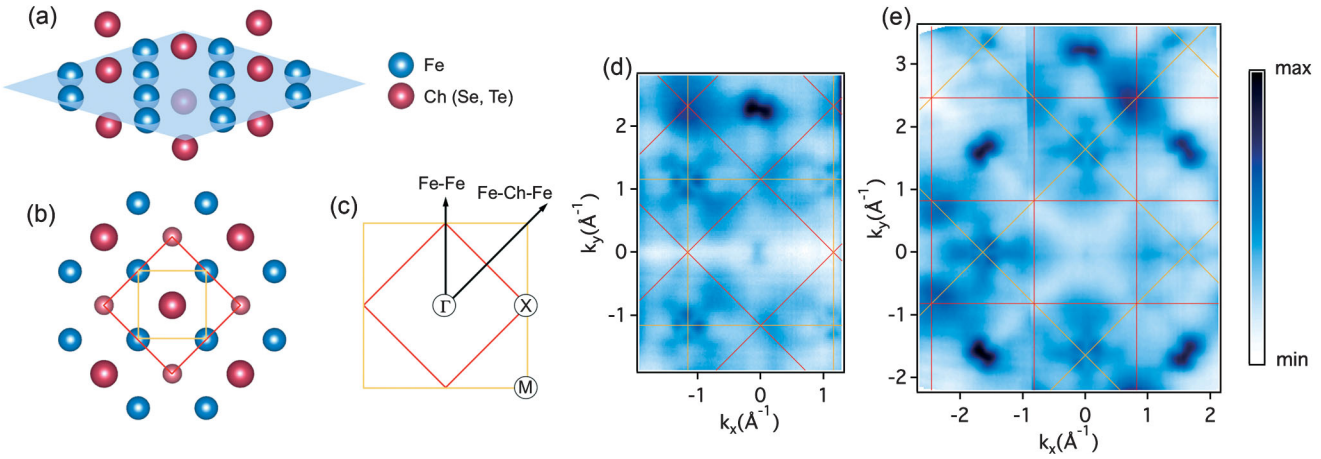

FIG. 1. (a) Three dimensional view of the $FeSe_xTe_{1-x}$ crystal structure, where nearest neighbor chalcogen atoms alternate above and below the Fe plane. (b) Projection onto the xy (Fe) plane. The size of the atoms is representative of the distance from the observer. The orange (red) square is the 1-Fe (2-Fe) unit cell. The corresponding Brillouin zones are shown in (c) with the same color code. (d) ARPES Fermi surface (FS) map of $Fe_{1.03}Se_{0.26}Te_{0.74}$ measured at 20 K with 140 eV photons and p polarization (for details see Ref. [4]). (e) Wide range FS map measured in the same experimental conditions as in (d), but after a 45° azimuthal rotation of the sample. Higher intensity is darker. No intensity normalization has been applied to the data.

wave vector range, in order to rule out dipole matrix element effects. By contrast, with a notable exception for a "122" pnictide [6], previous ARPES measurements have been limited to the first 2-Fe BZ.

Taking translational symmetry breaking at face value, all electronic states should exhibit the larger 2-Fe periodicity. The band structure calculated by standard density functional theory (DFT) would be folded into the smaller 2-Fe BZ, effectively doubling from 5 to 10 the number of (spin-degenerate) Fe $3d$ states. In a repeated zone scheme, the effect of a new periodicity is expected to be limited to replica features of the main bands, with intensity and hybridization gaps proportional to the size of the perturbing potential. Identical replica of the FS would, thus, also appear in all 2-Fe BZs. However, such a "geometrical" description, encountered, e.g., in charge density wave systems, is incomplete. Note also that the potential induced by the chalcogen atoms is not small, as clear gaps are formed at the 2-Fe BZ boundaries [5]. Therefore, the band structure is qualitatively different from that of a hypothetical crystal with the Te(Se) ions lying within the Fe plane.

The presence of two Fe atoms in the unit cell, responsible for the new periodicity, engenders in the photoemission matrix elements a structure factor term, which accounts for the wave function interference between the different atomic sites. Such a term is independent of the experimental conditions, such as direction and polarization of the incident light, and reflects instead intrinsic properties of the electronic structure. In fact, the spectral function $\tilde{A}(k, \omega)$, defined on the 1-Fe BZ, can be more directly compared with the intensity distribution $I(k, \omega)$ of an ARPES experiment [7]. The presence of a structure factor in $I(k, \omega)$ is inherent in the so-called one-step description of the technique [8–10], where it remains, nonetheless, implicit. As a consequence, it is almost always neglected at the stage of the data interpretation. To our knowledge, a thorough assessment of its role has been presented, so far, only for the cases of graphite or graphene [7,11,12], LiF [13] and Bi2212 [14].

Symmetry breaking in the Fe-based superconductors has been tackled by theory in two alternative ways. Since the two nonequivalent Fe ions are connected by a glide-mirror symmetry operation, the band structure was calculated in the 1-Fe BZ, at the price of adopting a "twisted," non-physical geometry [15]. Alternatively, bands can be unfolded into the larger 1-Fe BZ by explicitly including the symmetry breaking potential in the definition of the electron Green's function [5,16]. The second approach not only yields the energy-momentum band dispersion, but also assigns to all eigenvalues in the (1-Fe) BZ the proper spectral weight. The unfolded spectral function $\tilde{A}(k, \omega)$ encodes both the underlying 1-Fe periodicity and the perturbing potential [17]. Namely, it contains the structure factor of the (2-Fe) unit cell, i.e., the phase difference between the orbital wave functions of the two Fe ions.

Single crystals of $Fe_{1.03}Se_{0.26}Te_{0.74}$ with $T_c = 13$ K were grown by optical zone melting [18]. Samples were cleaved *in situ* to expose a clean (001) surface. ARPES measurements were performed at 20 K, in the normal state, at the Electronic Structure Factory, beam line 7.0.1 of the Advanced Light Source. The energy and momentum resolution of the hemispherical Scienta R4000 analyzer were 30 meV and 0.1°. DFT calculations within the local density approximation (LDA) were performed in the 2-Fe unit cell, solving the effective low-energy Hamiltonian defined via Fe d Wannier orbitals, and then unfolded as discussed in Ref. [16].

Figures 1(d) and 1(e) summarize the ARPES results. Figure 1(d) is an intensity map of the FS, measured with

140 eV photons, linearly polarized in the horizontal scattering plane. The value of k_z is close to that of a Γ point. All we discuss in the following is, however, independent on the exact value of k_z, and the pattern observed is reproducible at all the photon energies investigated [4]. Note also that the available momentum window is wider and the data are less sensitive to final state effects than in the UV range, where ARPES measurements are traditionally performed [14]. The k_y component of the wave vector was varied by rotating the sample about the horizontal x axis, which coincides with the Fe-Fe direction. Further details on the experimental geometry are available in Ref. [4], and for the following discussion, we note here that the data are presented without any intensity renormalization nor symmetrization. The orange square is the 1-Fe BZ, and in the following, we use the corresponding notation, namely for the $(M = \pi, \pi)$ and $(X = \pi, 0)$ points. Red squares in the figure outline the 2-Fe BZ in the reduced zone scheme. The map exhibits an intense feature at the adjacent Γ point, at $k_y = 2.32$ Å^{-1}, referred to as "butterfly" in the following. Fourfold ("cloverleaf") shapes are instead centered at the M points, the corners of the 1-Fe BZ. Further details on these features can be gained from constant energy cuts at various binding energies [4].

Figure 1(e) is a FS map measured over a broader momentum range, after a 45° rotation of the crystal around the surface normal, in order to align the ΓM direction with the horizontal axis. Butterfly shapes are now visible also at the centers of all the adjacent 1-Fe BZs. Each of them is perpendicular to the reflection symmetry plane identified by the corresponding k vector and the sample normal. Cloverleaf shapes are again observed at the M points. Note that the overall picture appears rotated by 45° with respect to Fig. 1(d), following the sample rotation, so that the lobes of the cloverleafs remain aligned with the edges of the BZ. The fact that the intensity pattern is locked to the azimuthal rotation of the sample rules out the dipole term of the matrix elements as the origin of the cloverleaf-butterfly dichotomy. In the 2-Fe scheme the Γ and M points are equivalent; i.e., they both correspond to the center of the 2-Fe BZ. However, the data of Fig. 1 show that their spectral signatures are very different. Clearly, a simple folding of the band structure into the smaller 2-Fe BZ does not adequately describe the electronic structure. This is our key experimental result, which we further discuss in the following.

Earlier DFT calculations have shown that the electronic structure of Fe(Se,Te) is similar to that of the Fe pnictides [19]. The FS consists of three concentric hole pockets at Γ and two electron pockets centered at the corner of the 2-Fe BZ, i.e., at the X point of the 1-Fe BZ. The butterfly and the cloverleaf ARPES features originate from the main and the replica hole pockets. The signatures of the electron FS sheets are weak and broad, as is usually the case in Te-rich samples [20–25]. Here, we focus on the hole FS sheets. Figures 2(a) and 2(b) present the calculated band structure for FeTe [26], projected on the Fe 3d orbitals, before (a) and after (b), unfolding it into the 1-Fe BZ. The corresponding FS are shown in Fig. 2(c) on the left and right side of Γ, respectively. The intensity scale is proportional to the spectral weight of each orbital character. Along the ΓM direction, the folded bands in (a) are symmetric with respect to the $(\pi/2, \pi/2)$ midpoint (the 2-Fe zone boundary) marked by a dashed line. By contrast, the unfolded band structure in (b) is not. Whereas the QP energies remain symmetric, not only is the total spectral weight markedly asymmetric with respect to the dashed line, e.g., weak at M and strong at Γ at the Fermi level, but also, the intensity of some orbitals is selectively suppressed on either side of $(\pi/2, \pi/2)$.

Qualitatively, the difference between panels 2(a) and 2(b), or equivalently between the two sides of panel (c), can be understood as follows [2]. The symmetry breaking potential is due to the staggered positions of the chalcogen ions above and below the Fe plane, along the z direction. Bands built from orbitals that are even with respect to a $\pm z$ reflection, such as d_{xy}, $d_{x^2-y^2}$, and $d_{3z^2-r^2}$, do not feel the doubled periodicity, and, therefore, will not generate a replica. The opposite is true for odd orbitals such as d_{xz} and d_{yz}. This can be extended to bands of mixed orbital character, where the weights of the even and odd components are switched between the main and replica bands. As a result, states at Γ and M exhibit opposite parities with respect to the Fe plane, e.g., $d_{3z^2-r^2}$ (cyan) and $d_{x^2-y^2}$ (yellow) at M, and $d_{xz} + d_{yz}$ (purple) at Γ.

We now consider, separately, the hole FS sheets formed at Γ and M. Butterfly shapes have been observed at the Γ point in the "11" compounds [22,24] and in LiFeAs [27]. They represent portions of the nearly circular hole FS contours selected by strong polarization effects, as illustrated in Fig. 2(d). The left side of Fig. 2(d) shows the calculated concentric hole contours generated by the d_{xy}, d_{xz}, and d_{yz} bands. The outer FS sheet has an essentially pure d_{xy} character. The two inner contours have mixed d_{xz}/d_{yz} character, and the weights of the d_{xz} and d_{yz} contributions are offset by 90°. Around Γ, the light polarization and the scattering geometry of our experiment select states of the d_{xz} character [2,4,22]. Therefore, the ARPES signal reproduces the d_{xz} part of the contours [right side of Fig. 2(d)], blurred by the finite energy and momentum resolution, and generates the butterfly shape. The two inner contours can be resolved away from the FS because the dispersion of the corresponding bands is different, and their separation increases with growing binding energy [4]. Similar considerations can be made for the horizontal butterfly feature in the second BZ and for those in all the adjacent BZs in Fig. 1(e). Here again, the light polarization selects the portions of the d_{xz}/d_{yz} contours that are oriented perpendicular to a reflection

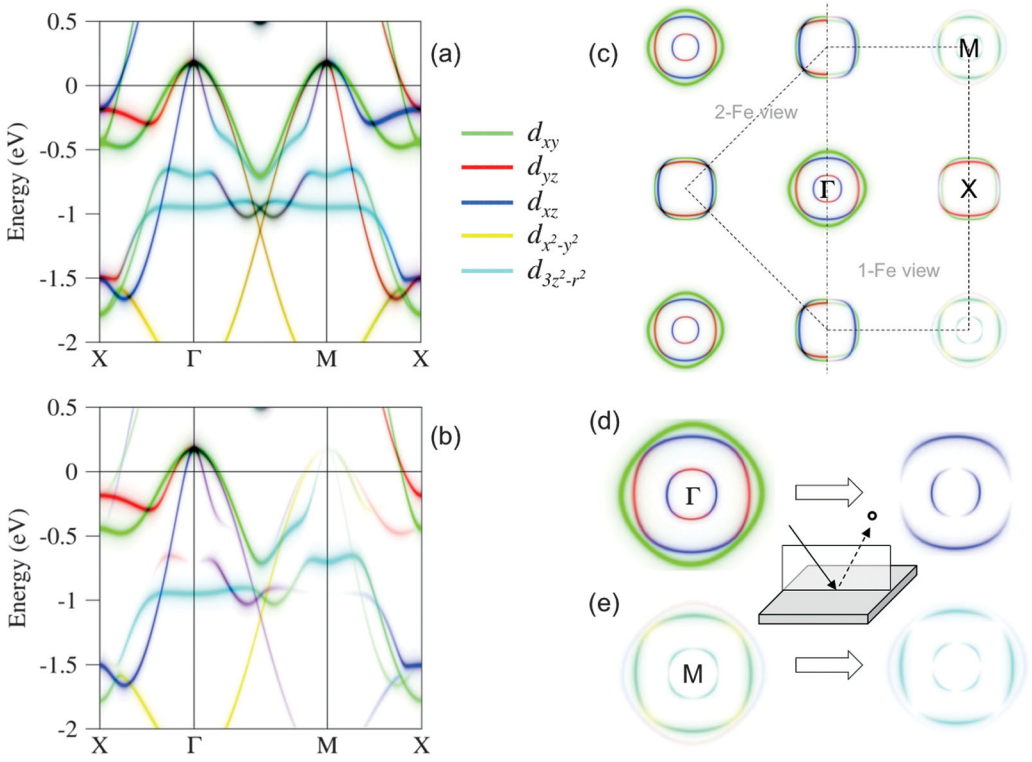

FIG. 2. (a) The spectral function $A(k,\omega)$, decomposed into the different orbital contributions. (b) Same as (a) for $\tilde{A}(k,\omega)$ unfolded from $A(k,\omega)$ onto the 1-Fe BZ. A constant lifetime is artificially included in the plot for visualization purposes, and the orbital character of each band is indicated by different colors. The computed bandwidth overestimates by a factor of ~5 the measured one due to well-known limitations of LDA. (c) FS for the 2-Fe unit cell (left) and 1-Fe unit cell (right), correspondent to the band structure in (a) and (b), respectively. The dashed lines indicate the corresponding BZ boundaries. Close-ups at Γ and M after unfolding onto the 1-Fe BZ are shown in [(d), left] and [(e), left], respectively. At Γ, the light polarization and experimental geometry select the d_{xz} component and generate the twofold butterfly [(d), right], at M they select the $d_{3z^2-r^2}$ character, and generate the fourfold cloverleaf [(e), right]. For a detailed discussion see Ref. [4]. In [(c), right] and (e), the $d_{3z^2-r^2}$ weight is amplified by a factor of 5.

symmetry plane, giving rise to the vortical pattern of butterfly shapes. We conclude that, (strong) polarization effects notwithstanding, the spectral features at the centers of all 1-Fe BZs are all equivalent.

The left side of Fig. 2(e) illustrates the calculated FS contours at M. The comparison with the cloverleaf shapes confirms the concept of parity switching proposed in Ref. [5], if we account for the dipole matrix element terms. The light polarization indeed again plays an important role, by selecting the $d_{3z^2-r^2}$ orbital character [4]. The weight of the $d_{3z^2-r^2}$ component along the FS contours at M [right side of Fig. 2(e)] has fourfold symmetry, with maxima along the Fe-Fe direction, consistent with the ARPES results.

An important distinction should be made between the case presented here and that of a quasi-one-dimensional system with an incommensurate superlattice potential discussed in Ref. [1]. In the latter, an emblematic single-orbital case, the perturbing potential can only change the magnitude of the hopping term, but clearly has no influence on the orbital character of the folded bands. On the other hand, when the system has higher dimensionality and more than one orbital is affected by the new potential, the conservation of the orbital character throughout the different BZs can no longer be taken for granted. In $FeSe_xTe_{1-x}$, the particular symmetry of the crystal allows exclusively for folding between orbitals of opposite parity, which leads to a characteristic inversion of the orbital symmetry in the "replica" bands, conclusively proved here by a broad ARPES survey of momentum space.

The present results reveal the importance of the typically overlooked structure factor in the spectral weight distribution measured in an ARPES experiment. They are readily extendable to the family of Fe pnictides, which exhibit similar band structures, and also to other spectroscopies, such as inelastic neutron scattering, where similar effects have been observed [28]. The parity switching demonstrated here and predicted by theory follows from the special symmetry of the perturbing potential, but we emphasize once more that orbital mixing can arise with folding whenever either the crystal structure or the electron distribution allow for the presence of multiple periodicities. Whether it is negligible, as in charge density wave systems, or substantial, as in this case, will depend on the form of the

symmetry-breaking potential, namely, on how it influences the hopping terms between the different orbital wave functions upon backfolding into the new Brillouin zone.

L. M. and P.-H. Lin equally contributed to this work. We gratefully acknowledge stimulating discussions with C. R. Ast, S. V. Borisenko, J. Denlinger, and H. M. Rønnow. We acknowledge support by the Swiss SNF, namely through Grant No. N PA00P21-36420 (L. M.). The Advanced Light Source is supported by the Director, Office of Science, Office of Basic Energy Sciences, of the U.S. Department of Energy under Contract No. DE-AC02-05CH11231. The Brookhaven National Laboratory is supported by the U.S. Department of Energy under Contract No. DE-AC02-98CH10886.

*lmoreschini@lbl.gov
†Present address: Institute of Physics, Academia Sinica, 128 Section 2, Academia Road, Nankang, Taipei 11529, Taiwan.phlinjoy@phys.sinica.edu.tw

[1] J. Voit, L. Perfetti, F. Zwick, H. Berger, G. Margaritondo, G. Grüner, H. Höchst, and M. Grioni, Science **290**, 501 (2000).
[2] V. Brouet, M. F. Jensen, P.-H. Lin, A. Taleb-Ibrahimi, P. Le Fèvre, F. Bertran, C.-H. Lin, W. Ku, A. Forget, and D. Colson, Phys. Rev. B **86**, 075123 (2012).
[3] D. C. Johnston, Adv. Phys. **59**, 803 (2010).
[4] See Supplemental Material at http://link.aps.org/supplemental/10.1103/PhysRevLett.112.087602 for experimental geometry and a detailed analysis of the polarization effects.
[5] C.-H. Lin, T. Berlijn, L. Wang, C.-C. Lee, W.-G. Yin, and W. Ku, Phys. Rev. Lett. **107**, 257001 (2011).
[6] V. B. Zabolotnyy, D. S. Inosov, D. V. Evtushinsky, A. Koitzsch, A. A. Kordyuk, G. L. Sun, J. T. Park, D. Haug, V. Hinkov, A. V. Boris *et al.*, Nature (London) **457**, 569 (2009).
[7] H. Daimon, S. Imada, H. Nishimoto, and S. Suga, J. Electron Spectrosc. Relat. Phenom. **76**, 487 (1995).
[8] J. Braun, Rep. Prog. Phys. **59**, 1267 (1996).
[9] F. Venturini, J. Minár, J. Braun, H. Ebert, and N. B. Brookes, Phys. Rev. B **77**, 045126 (2008).
[10] A. X. Gray, C. Papp, S. Ueda, B. Balke, Y. Yamashita, L. Plucinski, J. Minar, J. Braun, E. R. Ylvisaker, C. M. Schneider *et al.*, Nat. Mater. **10**, 759 (2011).
[11] E. L. Shirley, L. J. Terminello, A. Santoni, and F. J. Himpsel, Phys. Rev. B **51**, 13 614 (1995).
[12] M. Mucha-Kruczyński, O. Tsyplyatyev, A. Grishin, E. McCann, V. I. Fal'ko, A. Bostwick, and E. Rotenberg, Phys. Rev. B **77**, 195403 (2008).
[13] E. L. Shirley, L. J. Terminello, J. E. Klepeis, and F. J. Himpsel, Phys. Rev. B **53**, 10 296 (1996).
[14] M. Lindroos, S. Sahrakorpi, and A. Bansil, Phys. Rev. B **65**, 054514 (2002).
[15] O. K. Andersen and L. Boeri, Ann. Phys. (Berlin) **523**, 8 (2011).
[16] W. Ku, T. Berlijn, and C.-C. Lee, Phys. Rev. Lett. **104**, 216401 (2010).
[17] $A(k, \omega)$ and $\tilde{A}(k, \omega)$ were called $A_{KN,KN}$ and $A_{kn,kn}$ in Ref. [16], where $|KN\rangle$ and $|kn\rangle$ are the Fourier transform of Wannier orbitals for the reduced (2-Fe) and 1-Fe BZs, respectively.
[18] K. W. Yeh, C. T. Ke, T. W. Huang, T. K. Chen, Y. L. Huang, P. M. Wu, and M. K. Wu, Cryst. Growth Des. **9**, 4847 (2009).
[19] A. Subedi, L. Zhang, D. J. Singh, and M. H. Du, Phys. Rev. B **78**, 134514 (2008).
[20] Y. Xia, D. Qian, L. Wray, D. Hsieh, G. F. Chen, J. L. Luo, N. L. Wang, and M. Z. Hasan, Phys. Rev. Lett. **103**, 037002 (2009).
[21] Y. Zhang, F. Chen, C. He, L. X. Yang, B. P. Xie, Y. L. Xie, X. H. Chen, M. Fang, M. Arita, K. Shimada *et al.*, Phys. Rev. B **82**, 165113 (2010).
[22] F. Chen, B. Zhou, Y. Zhang, J. Wei, H.-W. Ou, J.-F. Zhao, C. He, Q.-Q. Ge, M. Arita, K. Shimada, *et al.*, Phys. Rev. B **81**, 014526 (2010).
[23] K. Nakayama, T. Sato, P. Richard, T. Kawahara, Y. Sekiba, T. Qian, G. Chen, J. L. Luo, N. L. Wang, H. Ding *et al.*, Phys. Rev. Lett. **105**, 197001 (2010).
[24] Y. Lubashevsky, E. Lahoud, K. Chashka, D. Podolsky, and A. Kanigel, Nat. Phys. **8**, 309 (2012).
[25] P.-H. Lin, Y. Texier, A. Taleb-Ibrahimi, P. Le Fèvre, F. Bertran, E. Giannini, M. Grioni, and V. Brouet, Phys. Rev. Lett. **111**, 217002 (2013).
[26] It is established that the band structures of FeTe and FeSe present quantitative, but not qualitative differences [see for instance A. Tamai *et al.*, Phys. Rev. Lett. **104**, 097002 (2010)]. Here, we present the case of FeTe, but our conclusions are completely general and do not rely on fine details of the calculated spectral function.
[27] S. V. Borisenko, V. B. Zabolotnyy, D. V. Evtushinsky, T. K. Kim, I. V. Morozov, A. N. Yaresko, A. A. Kordyuk, G. Behr, A. Vasiliev, R. Follath *et al.*, Phys. Rev. Lett. **105**, 067002 (2010).
[28] M. D. Lumsden, A. D. Christianson, E. A. Goremychkin, S. E. Nagler, H. A. Mook, M. B. Stone, D. L. Abernathy, T. Guidi, G. J. MacDougall, C. de la Cruz *et al.*, Nat. Phys. **6**, 182 (2010).